CENP-F Is a Protein of The Nuclear Matrix That Assembles onto Kinetochores at Late G2 and Is Rapidly Degraded After Mitosis

H. Liao,* R. J. Winkfein,‡ G. Mack,‡ J. B. Rattner,‡ and T. J. Yen*

*Fox Chase Cancer Center, Institute for Cancer Research, Philadelphia, Pennsylvania 19111; and ‡Department of Medical Biochemistry, University of Calgary, Calgary, Alberta, Canada T2N 4N1

Abstract. Centromere protein-F (CENP-F) is a mammalian kinetochore protein that was recently identified by an autoimmune serum (Rattner, J. B., A. Rao, M. J. Fritzler, D. W. Valencia, and T. J. Yen. *Cell Motil. Cytoskeleton.* 26:214–226). We report here the human cDNA sequence of CENP-F, along with its expression and localization patterns at different stages of the HeLa cell cycle. CENP-F is a protein of the nuclear matrix that gradually accumulates during the cell cycle until it reaches peak levels in G2 and M phase cells and is rapidly degraded upon completion of mitosis. CENP-F is first detected at the prekinetochore complex during late G2, and is clearly detectable as paired foci that correspond to all the centromeres by prophase. During mitosis, CENP-F is associated with kinetochores from prometaphase until early anaphase and is then detected at the spindle midzone throughout the remainder of anaphase. By telophase, CENP-F is concentrated within the intracellular bridge at either side of the midbody.

The predicted structure of the 367-kD CENP-F protein consists of two 1,600–amino acid-long coil domains that flank a central flexible core. A putative P-loop nucleotide binding site (ADIPTGKT) is located within the globular carboxy terminus. The structural features deduced from our sequence studies and the spatial and temperal distribution of CENP-F revealed in our cytological and biochemical studies suggest that it may play a role in several mitotic events.

THE kinetochore is a macromolecular structure that is associated with the centromeres of chromosomes and is responsible for establishing and maintaining the connections with the microtubules of the mitotic spindle. The kinetochore generates the force that is essential for the complex series of chromosome movements that lead to their alignment at metaphase and segregation at anaphase. Over the past ten years, efforts towards defining and characterizing the molecular composition of the centromere–kinetochore complex is slowly shedding new light on the molecular mechanism of chromosome segregation. Genetic analysis of the centromere DNA (CEN DNA)[1] in *Saccharomyces cerevisiae* has revealed a relatively simple *cis*-acting element of ~125 bp that is composed of the subdomains CDE I, II, and III (Clarke and Carbon, 1985). Biochemical analysis of the *trans*-acting factors that associate with CEN DNA has led to the purification of a heterotrimeric complex, CBF3 (Lechner and Carbon, 1991). In vitro, the CBF3:CEN DNA complex displays some kinetochore function as it exhibits motor activity that is directed towards the minus ends of microtubules (Hyman et al., 1992). The absence of any sequence similarity between the three CBF3 subunits to known microtubule-based motor proteins (Doheny et al., 1993; Goh and Kilmartin, 1993; Jiang et al., 1993) suggests that additional factors may be required for in vitro motility of the CBF3:CEN-DNA complexes. The discovery that the minus end-directed kinesin-like motor, KAR3p (Endow et al., 1994) is detected in substoichiometric levels in biochemically purified preparations of CBF3 (Middleton and Carbon, 1994) support the possibility that CBF3 functions as a scaffold upon which other components bind to form a functional yeast kinetochore.

Unlike *S. cerevisiae*, the chromosomes of higher organisms undergo a cell cycle-specific condensation–decondensation cycle that in part involves a protein family of hinge-like ATPases, the stability of mini chromosomes (SMC) family (Peterson, 1994). In addition, the DNA sequence and protein composition of the centromere–kinetochore complex in higher organisms are highly complex and the kinetochore has an extensive three-dimensional architecture that develops during chromosome condensation. Visually, the kinetochore can first be detected as a region of amorphous electron dense material at prophase (Brenner

Address all correspondence to T. J. Yen, Fox Chase Cancer Center, Institute for Cancer Research, 7701 Burholme Ave., Philadelphia, PA 19111. Tel.: (215) 728-4311. Fax: (215) 728-3616. E-mail: Yen@w462.xsome.fccc.edu.

1. *Abbreviations used in this paper*: cdk, cyclin-dependent kinases; CEN-DNA, centromere DNA; CENP, centromere protein; IPTG, isopropyl-thiogalactoside; MBP, maltose binding protein; SMC, stability of mini chromosomes.

et al., 1981). Subsequently, this material becomes organized into a trilaminar disk that obtains its final form at the surface of the centromere coinciding with the breakdown of the nuclear envelope. This tripartite structure persists until completion of cell division and the reformation of the interphase nucleus.

The discovery of a group of centromere proteins that associate with the centromere–kinetochore complex in both a cell cycle-dependent and -independent manner has been instrumental in providing the first insights into the molecular basis of centromere–kinetochore structure and function in higher organisms (Brinkley et al., 1992). Antibodies to the centromere proteins CENP A, B, and C (Earnshaw and Rothfield, 1985) have been used to visualize the position of the interphase prekinetochores (Brenner et al., 1981; Moroi et al., 1981). Furthermore, microinjection experiments using these antibodies support the notion that centromere–kinetochore assembly is a cell cycle-dependent process that is based upon the temporal interaction of multiple components of the centromere–kinetochore complex (Bernat et al., 1990, 1991). This conclusion has been further supported by the discovery of a subset of kinetochore proteins that transiently associate with the kinetochore as it matures. These proteins, in order of appearance include CENP-F (Rattner et al., 1993), CENP-E (Yen et al., 1991), p^{34cdc2} (Rattner et al., 1990), and dynein (Pfarr et al., 1990; Steuer et al., 1990).

CENP-F, first identified using human autoantibodies, is uniformly distributed in nuclei of cells that are in the late stages of the cell cycle during the onset of chromatin condensation. A subset of CENP-F abruptly localizes to the kinetochore during the period in which this structure first appears as a fuzzy ball of electron dense material. Subsequently, CENP-F is detected at the surface of the outer plate of the fully differentiated kinetochore (Rattner et al., 1993). After the onset of anaphase, CENP-F is found in the spindle midzone and subsequently within the intracellular bridge at either side of the midbody. In this report, we describe additional cell cycle studies and the molecular cloning of a CENP-F cDNA. The localization pattern of CENP-F together with its structural similarities to the emerging SMC family of chromosome compaction proteins suggest that it may play a role in organizing the interphase centromeric heterochromatin into highly differentiated trilaminar kinetochore complex at the onset of mitosis.

Materials and Methods

Cell Culture and Synchronization

HeLa cells were grown at 37°C in DMEM supplemented with 10% FCS and antibiotics. Synchronization of cells at the G1/S was performed by double thymidine block as described (Yen et al., 1992). Cells were released from the blocks by washing in warm PBS and replacing with complete growth media. Cell synchrony at various cell cycle stages was monitored by flow cytometry or by BrdU staining. For pulse labeling, cells were starved in cys^- and met^- serum-free medium for 20 min before addition of Tran^{35}S label (200 μCi/ml; ICN, Costa Mesa, CA) and 5% dialyzed FCS. Cells were labeled for 10 min before harvesting for immunoprecipitations. For pulse–chase experiments, cells that were synchronized at either G1/S or G2 were labeled for 15 min, washed, and then chased for 1, 2, and 4 h in unlabeled medium. For some experiments, pulse-labeled G2 cells were chased in medium that contained either 0.06 μg/ml colcemid (Sigma, St. Louis, MO) to block mitosis or in the presence of 5 mg/ml cytochalasin D (Sigma) to block cytokinesis. To obtain populations of HeLa cells that were highly enriched in G2, cells released for ~8 h from a G1/S block were rinsed to remove nonadherent mitotic cells and the remaining adherent G2 cells were used for pulse-labeling experiments or fixed and processed for antibody staining.

cDNA Cloning and Sequencing

5×10^5 phage from a λgt11 human breast carcinoma cDNA expression library (Clontech, Palo Alto, CA) was screened with VD autoimmune serum (Rattner et al., 1993) by following published protocols (Sambrook et al., 1989). Briefly, protein expression was induced by laying isopropylthiogalactoside (IPTG)-soaked nitrocellulose filters (Millipore, Bedford, MA) onto the phage-infected top agar. After 4 h at 37°C, filters were removed, rinsed, blocked and incubated overnight at 4°C with VD serum (1:500). Filters were washed the next morning, and bound antibodies were detected with ^{125}I-protein A (1:2,500; ICN). Positive plaques were eluted and rescreened with the autoimmune serum until single plaques were identified. For plaque hybridizations, 3×10^6 plaques from the same cDNA library were screened with a 300 bp EcoRI and HindIII fragment that was derived from the 5′ end of clone D7. Probes were labeled to high specific activity with α^{32}P dCTP (Amersham, Arlington Heights, IL) by random priming. Filters were hybridized at 60°C in aqueous buffer (5× SSPE, 5× Denhardt's, 0.5%SDS, 100 μg/ml of sonicated herring sperm DNA) containing 5×10^5 cpm/ml of probe. Filters were washed at high stringency (65°C in 0.2× SSC, 0.1% SDS for 20 min) before exposing to x-ray film.

cDNAs were isolated from the recombinant phage DNA by either EcoRI or BsiWI digestion, subcloned into the EcoRI or Acc65I sites in either the vectors M13 mp18 or pBluescript SK. 5′RACE was performed with HeLa poly(A)$^+$ mRNA using Amplifinder kit (Clontech, Palo Alto, CA.). To increase specificity, nested primers TJY42, 5′-CTTTTGCTTTCTCCAGTTGG-3′ and TJY43, 5′-TTGACGCCTGGTCGTATTG-3′, were used for the RT-PCR. The complete cDNA was determined from both strands by sequencing overlapping restriction fragments. DNA sequencing was performed with Sequenase v2.0 (USB, Cleveland, OH). Compilation and analysis of the DNA sequences were performed either with MacVector (Kodak) or GCG (University of Wisconsin, Madison, WI). Database searches were performed with BLAST (Altschul et al., 1990) and predictions of coiled coil formation was performed with the COILCOIL program (Lupas et al., 1991).

Northern Blots

2 to 3 μg of HeLa poly(A)$^+$ mRNA that was isolated from cells enriched in the G2 stage of the cell cycle was separated by electrophoresis in a formaldehyde agarose gel, transferred onto Hybond N (Amersham) and the filter was processed according to manufacturer's instructions. EcoRI fragments derived from the different cDNA isolates were individually hybridized to the filters under the hybridization conditions described above.

Bacterial Fusion Protein Expression and Generation of CENP-F Antibodies

EcoRI fragments that spanned different portions of CENP-F cDNA (from nucleotide 3420 to 6408, 6992 to 7538, and 8445 to end) were subcloned into the expression vector pMAL (New England Biolabs, Beverly, MA) and transformed into *E. coli* strain CAG456. Protein expression was induced with 1 mm IPTG when cultures reached an OD_{600} of 0.6. After 4 h at 30°C, bacteria were harvested, washed and sonicated. The S30 fraction that contained the fusion protein was immediately frozen or boiled in SDS sample buffer, and the proteins separated by SDS PAGE. Fusion protein was sliced from the gel after staining in 0.1% Coomassie Brilliant Blue and 40% methanol. Macerated gel slices containing between 100 to 200 μg of fusion protein were injected into rabbits. Each rabbit was boosted twice (2–3 wk between boosts) before serum was tested by immunofluorescence staining and immunoblotting. Rabbit IgG was purified by ion exchange chromatography, concentrated with a Microcon 30 (Amicon, Beverly, MA) to ~5–10 mg/ml in PBS.

Immunodetection Methods

For immunofluorescence staining, HeLa cells growing on 18 mm coverslips were fixed at RT for 5 min in 3.5% paraformaldehyde buffered in PBS at pH 6.8, extracted for 5 min in KB+0.2% Triton X-100 (KB: 50 mM

Tris-HCl, pH 7.4, 150 mM NaCl, 0.1% BSA), rinsed in KB for 10 min and then incubated with CENP-F IgG in a 37°C humidified chamber. After 1 h, coverslips were washed in KB for 10 min and incubated with 5 μg/ml FITC coupled goat anti-rabbit (GIBCO BRL, Gaithersburg, MD) for 30 min. For double immunofluorescence, bound human IgG was incubated with 1 μg/ml biotinylated anti-human IgG followed by incubation in 1 μg/ml streptavidin-Texas Red. Nuclei and chromosomes were stained with 4′,6′ diamino phenylindole (DAPI; Sigma) at 0.1 μg/ml. No significant difference was observed when samples were fixed directly in −20°C methanol. Coverslips were mounted in Vectashield (Vector, Burlingame, CA) and observed with a Nikon Microphot SA equipped with epifluorescence optics. Images were observed with a 100X Plan Neofluor objective and photographs were recorded on Tmax400 film (Kodak).

For immunoprecipitation, HeLa cells were harvested, washed and lysed either in RIPA buffer (50 mM Tris-HCl, pH 7.5, 150 mM NaCl, 1% Triton X-100, 1% deoxycholate, 0.2% SDS) or EBC buffer (50 mM Tris-HCl, pH 7.5, 200 mM NaCl, 0.5% NP-40) in the presence of protease inhibitors (1 mm PMSF, 1 mm benzamidine, 10 μg/ml leupeptin, 10 μg/ml pepstatin). Immunoprecipitations were performed by incubating autoimmune serum (1:200) or rabbit CENP-F IgG (1:200) with clarified lysates at 4°C for several hours. Immunocomplexes were precipitated with 30 μl of a 1:1 slurry of protein A–Sepharose beads (Pharmacia, Piscataway, NJ), washed, boiled in SDS sample buffer and separated by SDS PAGE. For detection of ^{35}S-labeled proteins, the gels were fixed and enhanced in 1 M salicylate before drying and exposing to x-ray film (Kodak XAR). For immunoblot analysis, separated proteins were transferred onto Immobilon P (Millipore, Bedford, MA), blocked, incubated with autoimmune (1:500) or anti-CENP-F IgG (1:500) as described (Yen et al., 1991). Bound antibodies were detected with ^{125}I-protein A (ICN) or by chemiluminescence (Bio-Rad Labs., Richmond, CA).

Preparation of Nuclear Matrix

Nuclear matrices were prepared essentially as described (Staufenbiel and Deppert, 1984) except that the final DNase and RNase digestions were omitted in order to preserve the nuclear core filaments (He et al., 1990). For biochemical fractionation, HeLa cells were harvested from dishes by cell dissociation solution (Sigma) and washed three times with KM buffer (10 mM N-morpholinoethanesulfonic acid, pH 6.2, 10 mM NaCl, 1.5 mM MgCl2, 10% glycerol, 30 μg/ml aprotinin). Cell pellets were first extracted with KM buffer containing 1% NP-40, 1 mM EGTA, and 5 mM DTT at 4°C for 20 min. The extracted cytoplasm was saved and the remaining nuclei were washed three times with KM buffer and then digested with DNase I (100 μg/ml) in KM buffer at 37°C for 30 min. The supernatant was saved and the pellet was washed once, and extracted further with KM buffer containing 2N NaCl, 1 mm EGTA, and 5 mM DTT at 4°C for 30 min. The nuclear matrix pellet was solubilized with RIPA buffer (50 mM Tris, pH 8, 150 mM NaCl, 0.5% DOC, 0.1% SDS, 1% NP 40, 30 μg aprotinin) and brief sonication. A RIPA lysate of unextracted cells was used to monitor efficiency of recovery of CENP-F in the extracted samples. CENP-F was immunoprecipitated from all fractions and detected by immunoblots using CENP-F antibodies. For immunofluorescence staining, cells grown on coverslips were enriched for G2 population by releasing for 6 h after a single thymidine block. Cells were washed three times with KM buffer and sequentially incubated with KM containing 1% NP 40, DNase I and 2N NaCl as described above. After the final extraction, coverslips were washed with KM buffer and fixed in −20°C methanol for 10 min followed by −20°C acetone for 5 min. Unextracted cells were directly fixed in methanol/acetone. Immunofluorescence was performed as described above.

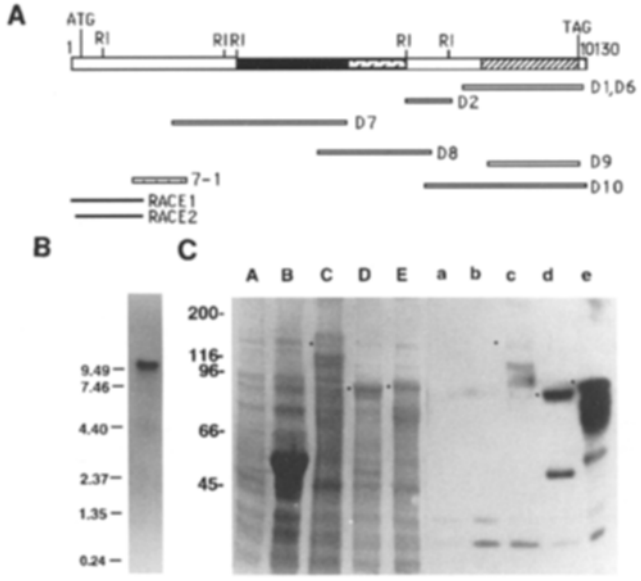

Figure 1. Autoimmune serum identifies overlapping cDNAs that encode multiple epitopes. (*A*) Schematic diagram depicting overall cloning strategy. The three regions of the cDNA that were used to generate antibodies are indicated by the three different cross-hatch patterns. (*B*) Representative Northern blot of HeLa mRNA using the 2.8-kb D10 cDNA as probes. RNA size standards are shown on the left. (*C*) (*Left*) Coomassie stained gel of bacterial lysates from: lane *A*, uninduced culture; lanes *B–E*, induced cultures that expressed MBP:7L, MBP:8L, and MBP:D10. (*Right*) Immunoblot of the identical samples (lanes *a–e*) using VD autoimmune serum (1:500). (*) Migration position of the full-length MBP fusion proteins.

Results

Autoimmune Serum Identifies Overlapping cDNAs That Express Cross-reactive Epitopes

Eight immunopositive phage clones (D1, D2, and D5 through D10) were isolated after screening a human cDNA expression library with VD autoimmune serum that contained CENP-F antibodies (Rattner et al., 1993). Restriction mapping and inspection of partial DNA sequences of the various clones revealed that they were all related (Fig.1 *A*) with the exception of clone D5 that was not further characterized. Clones D7, D8, and D10 overlapped one another and spanned 8.3 kb of contiguous

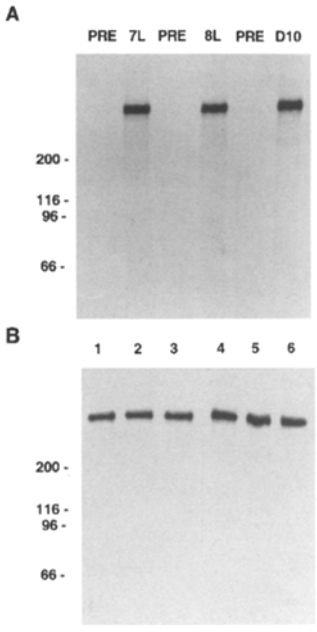

Figure 2. Rabbit polyclonal antibodies generated against proteins expressed from three different regions of CENP-F recognize CENP-F from HeLa cells. (*A*) Immunoblot of mitotic HeLa cell lysates with rabbit polyclonal antibodies raised against CENP-F fusion proteins 7L, 8L, D10, and their corresponding preimmune IgG (*PRE*). (*B*) Mitotic cell lysates were immunoprecipitated with autoimmune serum (lanes *1–3*) and probed with rabbit polyclonal antibody 7L, 8L, D10 in lanes *1*, *2*, and *3*, respectively. Conversely, immunoprecipitates obtained with antibodies 7L, 8L, or D10 in lanes *4*, *5*, and *6*, respectively, were probed with VD autoimmune serum. The molecular mass markers are shown on the left.

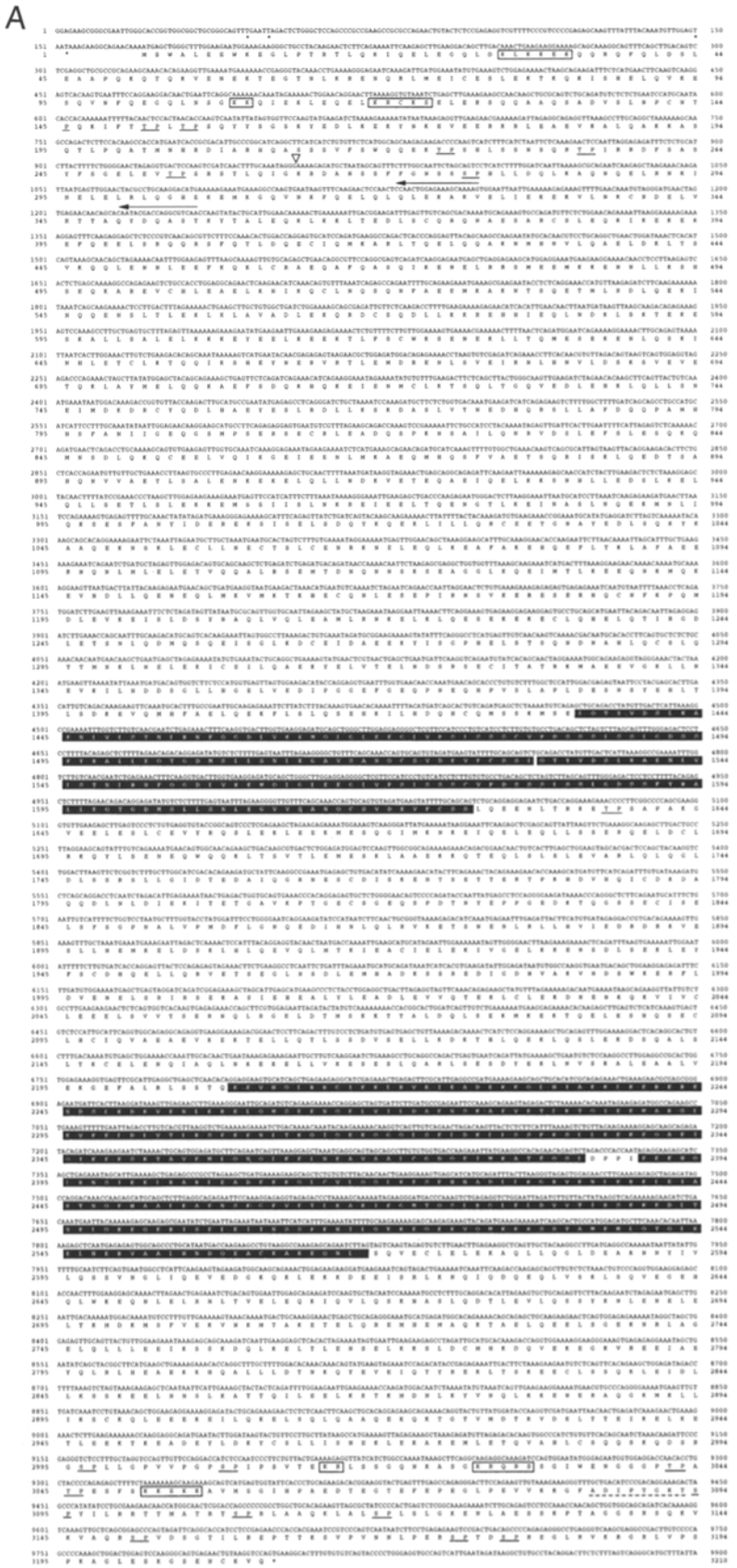

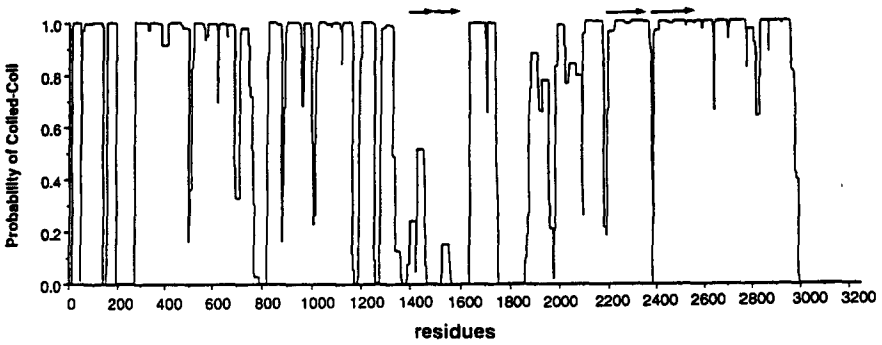

Figure 3. Primary and predicted secondary structure of CENP-F. (*A*) DNA sequence of the CENP-F cDNA and its predicted amino acid sequence. Underline, consensus cdk and MAP kinase phosphorylation sites; dashed line, consensus P-loop NTP binding motif; box, bipartite and conventional nuclear localization sequence; white characters, the two pairs of direct repeats; asterisk, termination codon. Arrows, nested primers TJY42 and TJY43 that were used for 5'RACE. Open triangle, 5' boundary of the phage clone 7-1. (*B*) Probability plot of coil formation of CENP-F as predicted by the COILCOIL program using the maximal window size of 24 (Lupas et al., 1991). Arrows above the plot depict the positions of the two direct repeats. These sequence data are available from EMBL/Genbank/DDBJ under accession number U19769.

cDNA that included a long poly A tail at the 3' end. Since all three clones contained multiple EcoRI fragments, we tested whether they might be derived from the same mRNA by using each fragment to probe filters that contained HeLa poly(A)$^+$ mRNA. Consistent with this possibility, all of the fragments hybridized to a single, 10–11-kb RNA (Fig. 1 *B*) that was of the appropriate size to encode the estimated 400-kD CENP-F protein.

To verify whether the initial set of phage clones encoded CENP-F, three cDNA fragments derived from clones D7, D8, and D10 were subcloned into the expression vector pMAL for protein expression in *E. coli*. Each of the cDNA fragments expressed a fusion protein of the expected size (172, 82, and 96 kD) as well as a cluster of smaller proteolytic fragments (Fig. 1 *C*, *A–E*). The sensitivity to proteolysis may be due to the general observation that proteins with extensive helical structure are highly unstable in bacteria. Immunoblot analysis using VD autoimmune serum showed that it did not identify any proteins of comparable size to that of the three maltose binding protein (MBP):CENP-F fusion proteins in uninduced bacterial extracts, or an extract containing MBP (Fig. 1 *C*, lanes *a* and *b*). However, the VD autoimmune serum recognized all three MBP:CENP-F fusions as well as a number of degradation products (Fig. 1 *C*, lanes *c–e*). Since the MBP did not express epitopes recognized by the autoimmune serum, reactivity must be directed against epitopes that are encoded by the three different cDNA fragments. The low molecular mass immunoreactive bands that appear in all the lanes is due to cross-reactivity between the autoimmune serum and some endogenous bacterial proteins. Preabsorption of autoimmune serum with uninduced bacterial extracts significantly reduced the intensity of these bands in subsequent immunoblots (data not shown).

Authentication of CENP-F cDNAs

To directly verify the authenticity of these various cDNAs, antibodies were generated against the MBP:7L, MBP:8L, and MBP:D10 fusion proteins (Fig. 1 *A*). Rabbit sera that recognized the injected fusion proteins by immunoblot analysis were tested for their ability to recognize the CENP-F protein that was present in HeLa cells. Immunoblot analysis of HeLa mitotic cell lysates showed that while none of the pre-immune antibodies detected a protein of the size of CENP-F, all three antibodies identified a single protein whose size was very similar to CENP-F (Fig. 2 *A*). To directly test whether these antibodies recognized CENP-F, autoimmune serum was used to immunoprecipitate CENP-F from HeLa cells and the immunocomplexes were probed with the three different antibodies by immunoblot analysis (Fig. 2 *B*, lanes *1–3*). Conversely, immunoprecipitates obtained with the three rabbit antibodies were probed with the autoimmune serum (Fig. 2 *B*, lanes *4–6*). Both approaches demonstrated that antibodies raised against the various bacterial fusion proteins recognized CENP-F in HeLa cells. Given that the cDNAs encode multiple epitopes that are recognized by VD autoimmune serum, and that the proteins expressed from these cDNAs elicited antibodies that recognized CENP-F, these results confirmed that we had isolated portions of the authentic CENP-F cDNA.

Isolation of a cDNA That Encodes for a Full-length CENP-F

Exhaustive screening of a cDNA library by plaque hybridization yielded several clones, one of which extended the existing 8.3 kb of cDNA by ~0.75 kb towards the 5' end (Fig. 1 *A*, clone *7-1*). Since the open reading frame that was derived from the 9 kb of contiguous of DNA sequence was still insufficient to account for the estimated 400-kD size of CENP-F, the cDNA was extended further towards the 5' end by 5'RACE. We isolated poly(A)$^+$ mRNA from cells synchronized at the G2 stage, when CENP-F RNA levels were highest (T. J. Yen, unpublished observations), and used a pair of nested oligonucleotide primers that were near the 5' end of clone 7-1 to perform RT-PCR (Fig. 3 *A*). PCR products that extended the cDNA by another 1.1 kb were obtained. DNA sequence of several independent PCR clones revealed a region of perfect overlap that began at the nested primer and extended to the 5' end of clone 7-1. The presence of this extended region of overlap confirmed that the RACE products were amplified from CENP-F mRNA. Finally, Northern blots showed that the RACE products identified the same size RNA as was identified by the other cDNA fragments (data not shown).

Two 5' RACE products that differed in length by 42

base pairs at their 5′ ends were isolated and sequenced. The shorter RACE fragment was presumably derived from a prematurely terminated product from the first-strand cDNA synthesis reaction. The difference in length between these two RACE products did not alter the coding capacity of the remainder of the cDNA as translation must initiate from the same ATG to express a protein of the appropriate size. Inspection of the 10,142-bp CENP-F cDNA sequence (Fig. 3 *A*) revealed that if translation initiated at position 171, a polypeptide of 3210 amino acids with a calculated mass of 367 kD would be produced. Given that the sequence upstream of the putative translation initiation codon cannot extend the open reading frame due to the presence of multiple termination codons and that the calculated mass is close to the estimated size of 400 kD, we conclude that the complete coding sequence of CENP-F was cloned.

Analysis of the Primary and Predicted Secondary Structure of CENP-F

The primary sequence of CENP-F (Fig. 3 *A*) did not exhibit any significant homologies with other known proteins in the database. However, CENP-F consistently exhibited a low level of homology (<20%) with the rod domains of many cytoskeletal proteins such as myosins, kinesins, lamins, and tropomyosins that probably reflected similarities in secondary structure. Analysis of the CENP-F amino acid sequence with the COILCOIL program (Lupas, 1991) showed that a significant portion of the protein had a high probability of forming an extended coil (Fig. 3 *B*, residues 1–200, 280–1350, 1620–1750, 1850–2990). Upon further inspection, CENP-F was found to contain two pairs of direct repeats. A 96–amino acid repeat was positioned in between the two largest coil domains, and a 178–amino acid direct repeat was located within the last coil domain (Fig. 3 *A*, *bracketed*). Neither set of repeats contained any recognizable motifs or exhibited homologies with other proteins.

Examination of the charge distribution in CENP-F showed that the extended central rod domain has an overall calculated pI of ~5.2. This contrasts with the predicted pI's of the amino and carboxyl 200–amino acid domains of 9.1 and 10, respectively. Additional motifs that are found in common between the amino and carboxy termini include bipartite as well as conventional consensus nuclear localization sequences (Fig. 3 *A*, *boxes*) and clusters of consensus phosphorylation sites for either MAP kinases or cyclin-dependent kinases (cdk) (Fig. 3 *A*, *overlines*). The carboxyl terminus exhibited two additional distinguishing features that include a high proline content (10.6%), and the sequence, ADIPTGKT, that fits the type A motif of NTP binding sites (A/G)XXXXGK(S/T) (Walker et al., 1982; Fry et al., 1986; Linder et al., 1989; Saraste et al., 1990).

CENP-F Is a Component of the Nuclear Matrix during Interphase

CENP-F is distributed uniformly in the interphase nucleus at early stages of G2 (see below) but exhibits a granular staining pattern. To examine whether CENP-F might be associated with the nuclear matrix, HeLa nuclei were successively extracted with 1% NP-40, DNase I digestion, and 2 M NaCl to obtain a nuclear matrix. Since the presence of RNA has been shown to be essential for maintaining the core filament organization of the nuclear matrix (He et al., 1990), the final step of DNase I/RNase A digestion was omitted from the original protocol to preserve the architecture of the nuclear matrix. To ensure the complete removal of the chromatin, the time of DNase I digestion was prolonged. As shown in Fig. 4 *E*, DAPI staining was completely abolished in our nuclear matrix preparations. To quantitate the recovery of CENP-F at each extraction step, CENP-F was immunoprecipitated and analyzed by immunoblotting. Comparison with unextracted cells showed that the majority of CENP-F was enriched in the nuclear matrix preparation (Fig. 4 *A*, compare lane *1* with *5*) while only a small portion was detected in the three soluble fractions (Fig. 4 *A*, lanes *2–4*). In contrast to interphase cells, a large proportion of CENP-F was detected in the soluble fraction after gentle permeabilization of mitotic cells (Fig. 4 *A*, lanes *6* and *7*). The release of CENP-F into the mitotic cytoplasm (see Fig. 7) is consistent with the breakdown of the nuclear matrix at mitosis. In support of the biochemical data obtained on interphase cells, the im-

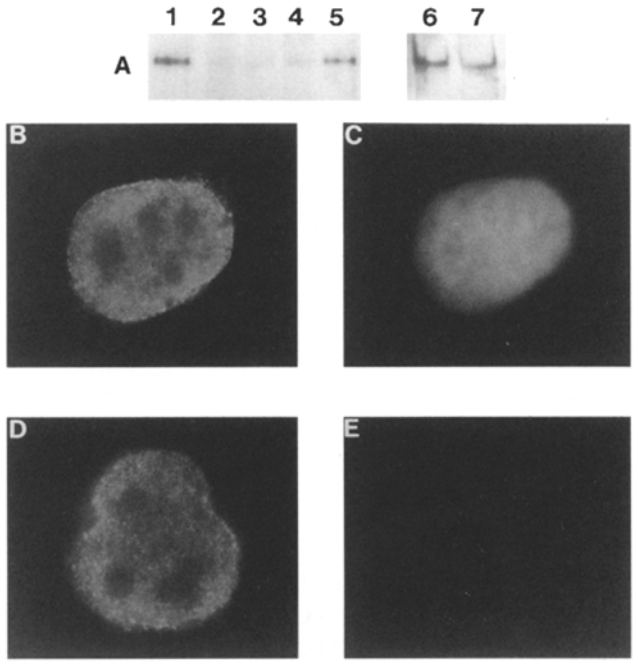

Figure 4. CENP-F is a component of the nuclear matrix that becomes partially solubilized at mitosis. (*A*) Interphase HeLa cells were successively fractionated into cytoplasm (lane *2*), nuclear extract after DNase I digestion (lane *3*), 2 M NaCl extract (lane *4*), and nuclear matrices (lane *5*). The total cell lysate (lane *1*) from an equal number of cells as was used in nuclear matrix preparation served as control for efficiency of recovery of CENP-F. Mitotic cells were extracted with EBC buffer to separate soluble proteins (lane *6*) from insoluble complexes (lane *7*) such as chromosomes. Each fraction was solubilized or diluted into with RIPA buffer after sonication, immunoprecipitated with antibody 7L, and analyzed by immunoblot. (*B–E*) Immunofluorescence staining of a control unextracted cell (*B* and *C*) and in situ prepared nuclear matrices (*D* and *E*) stained with antibody 7L and counterstained with FITC-conjugated anti-rabbit IgG (*B* and *D*) and DAPI (*C* and *E*).

munofluorescence staining of the nuclear matrix with CENP-F antibodies showed nearly the same intensity as that which was detected in a control unextracted nucleus (Fig. 4, compare *B* with *D*). Furthermore, the distribution pattern of CENP-F was unaltered by nuclease digestion, and detergent and salt extractions as it remained uniformly distributed throughout the non-nucleolar regions in a fine granular pattern (Fig. 4, compare *B* with *D*). The combined data suggest that CENP-F is a component of the nuclear matrix.

CENP-F Localization Changes during the Interphase and Mitotic Cell Cycles

Previous data obtained with autoimmune serum showed that CENP-F is a nuclear protein that is detected in only some interphase cells (Rattner et al., 1993). This observation suggested that CENP-F expression and localization may be cell-cycle dependent. To obtain a more accurate estimate of when CENP-F is detectable during the cell cycle, we used the D10 CENP-F antibodies to stain synchronized HeLa cells. Neither preimmune IgG or immune IgG that was preincubated with the MBP:D10 fusion protein produced any significant staining above background (data not shown). CENP-F was not detectable in cells in early G1 (Fig. 5 *B*) or shortly after release from the G1/S boundary (data not shown). As cells progressed through S phase (as monitored independently by BrdU staining), weak nuclear staining was detectable (data not shown). In G2 cells, very bright CENP-F staining was detected uniformly throughout the nucleus but was excluded from nucleoli (Fig. 5 *E*). In some cases, G2 nuclei also exhibited bright CENP-F staining around the nuclear boundary (Fig. 5 *F*). As shown below, the nuclear rim staining is observed in cells that were in the late stages of G2.

We also estimated the earliest time when CENP-F could be detected at centromeres by increasing our sampling frequency of synchronized cells that were progressing through G2. In late G2 cells, the uniform nuclear distribution of CENP-F gave way to localization around the nuclear boundary and multiple bright paired foci within the nucleus (Fig. 6, *B* and *E*). These cells were estimated to be in late G2 by observing that a parallel culture of cells entered into mitosis within 60 min from the time that these cells were processed for staining. Double staining with ACA sera (Fig. 6, *C* and *F*) confirmed that the foci of CENP-F staining were coincident with centromeres. Closer inspection showed that not all the centromeres of these cells exhibited CENP-F staining, perhaps reflecting the asynchronous maturation of the centromere-kinetochore complex. By prophase (Fig. 6 *G*), CENP-F is clearly present at all the centromeres as discrete pairs of foci (Fig. 6 *H*). Since fully formed kinetochores are not detectable until the onset of nuclear envelope breakdown, CENP-F should be considered to be localized at prekinetochores at this time. The assembly of CENP-F at prekinetochores correlated with a general reduction in nuclear staining (compare the intensity of nuclear staining of CENP-F in Fig. 6, *B*, *E*, and *H*). The reduction in nuclear staining was also accompanied by increased chromatin condensation (Fig. 6, *A*, *D*, and *G*). Finally, the intensity of the nuclear rim staining was noticeably diminished as cells progressed closer to mitosis and the continuous band of staining around the nucleus was highly perforated by prophase (Fig. 6 *H*).

We next examined the distribution pattern of CENP-F at different stages of mitosis. As shown above, CENP-F is detectable at the pre-kinetochores of prophase chromosomes (Fig. 7 *B*). CENP-F was associated with kinetochores in prometaphase and metaphase cells (Fig. 7, *D* and *F*) and was still detectable at kinetochores after the onset of sister chromatid separation in early anaphase. By late in anaphase, staining was relatively diffuse throughout the cell with the exception of a distinct, narrow stripe of staining at the spindle equator (Fig. 7 *J*). The narrow stripe of staining became concentrated into the intracellular bridge as a result of cleavage furrow formation during cytokinesis (Fig. 7 *L*). The majority of CENP-F is degraded (see below) after cells complete mitosis since only background staining is detectable in early G1 cells. Besides detecting the presence of CENP-F at different structures during the different stages of mitosis, CENP-F was also found throughout the cytoplasm of mitotic cells. This observation confirms the biochemical data that showed a large fraction of CENP-F became soluble during mitosis.

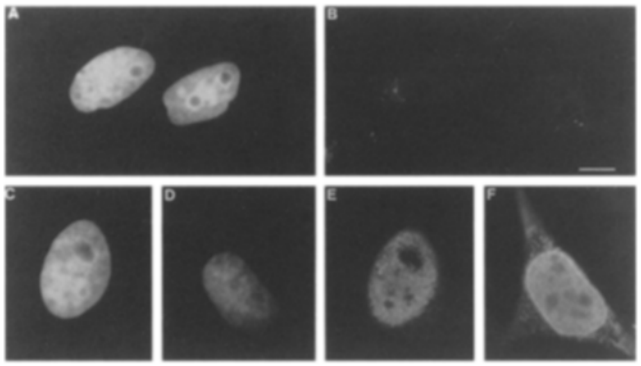

Figure 5. CENP-F is a nuclear protein that accumulates to peak levels in G2 stage of the cell cycle. HeLa cells in early G1 (*A* and *B*) or in G2 (*C* through *F*) were fixed and stained with DAPI (*A*, *C*, and *D*) and CENP-F antibodies (*B*, *E*, and *F*). Primary antibody was visualized with FITC-conjugated anti-rabbit IgG. Bar, 10 μm.

Quantitation of the Expression Patterns of CENP-F at Different Cell Cycle Stages

The immunofluorescence staining pattern of CENP-F suggested that its expression pattern was cell cycle regulated. To quantitate the cell cycle expression pattern of CENP-F, we first compared the steady-state levels of CENP-F in cells that were synchronized at various parts of the cell cycle (Fig. 8 *A*). Consistent with the absence of CENP-F staining in G1 cells, immunoblot analysis showed low levels of CENP-F in cells that were synchronized at the G1/S boundary. CENP-F steady-state levels gradually increased as cells progressed through S phase and reached peak levels at G2 and M. CENP-F steady-state levels dropped dramatically after cells completed mitosis and reentered G1. Considering that the early G1 fraction was contaminated with a small amount (8–12% by flow cytometry) of G2 cells, the 15-fold loss in CENP-F between M phase and early G1 cells is an underestimate. Consistent with the rise

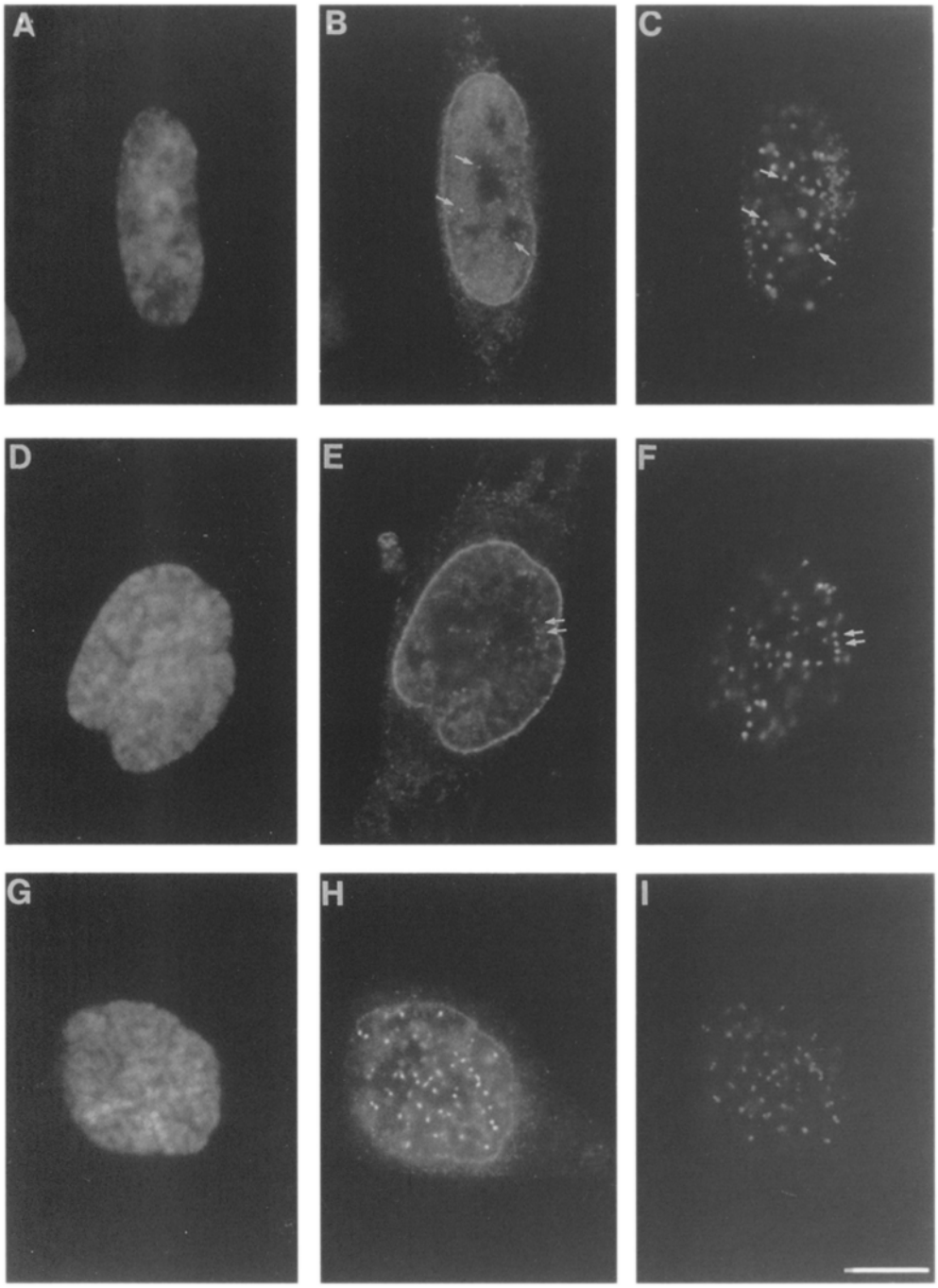

Figure 6. CENP-F is detected at prekinetochores at late G2 when chromatin condensation is detected. 9.5 h after release from the G1/S boundary, mitotic cells were removed by shakeoff and the remaining adherent cells were fixed and stained with DAPI (*A*, *D*, and *G*), anti-CENP-F IgG (*B*, *E*, and *H*), and ACA serum (*C*, *F*, and *I*). DAPI was used at 0.05 μg/ml to reveal details of chromatin condensation. The degree of chromatin condensation was used to assign proximity of the three cells to mitosis. CENP-F antibodies were visualized with FITC-conjugated anti-rabbit IgG and ACA was detected with streptavidin-Texas Red that was bound to biotinylated anti-human IgG. Each row of images were obtained at the same focal plane. Equivalent exposure times were used for each channel to allow comparison of relative staining intensities of CENP-F amongst the three cells. Arrows point to colocalization of CENP-F and ACA. Bar, 10 μm.

in the steady-state levels during S and G2, the synthetic rate of CENP-F increased threefold as cells progressed from S and peaked during G2 (Fig. 8 *B*).

The 15-fold increase in the steady-state level of CENP-F in G2 cells with only a modest threefold elevation in its synthetic rate could only be accounted if its turnover rate was slow. On the other hand, the dramatic loss of CENP-F at the end of mitosis would require that the degradation of CENP-F be accelerated. To test whether protein stability played a role in regulating the steady-state levels of CENP-F during the cell cycle, the turnover rate of CENP-F was determined at different cell cycle stages. We initially established the rate of CENP-F turnover in interphase by examining cells that were progressing from the G1/S boundary through S phase. Cells synchronized at the G1/S boundary were pulse labeled and then chased for 4 h through S phase (Fig. 9 *A*). A plot of the amount of radiolabeled CENP-F at various times during the chase showed the $t_{1/2}$ to be ~4.6 h (Fig. 9 *D*). Analysis of the turnover rate of CENP-F when cells were progressing from G2 through mitosis revealed a biphasic decay curve (Fig. 9, *B* and *D*). During the first hour of the chase, when most cells were still in G2 and M, the $t_{1/2}$ was similar to that observed earlier in the cell cycle. However, over the next hour, when the vast majority of the cells had progressed through mitosis and into G1, the $t_{1/2}$ was reduced fivefold to 0.9 h. The slower rate of CENP-F decay after 4 h of chase was likely due to contamination of the predominantly G1 population

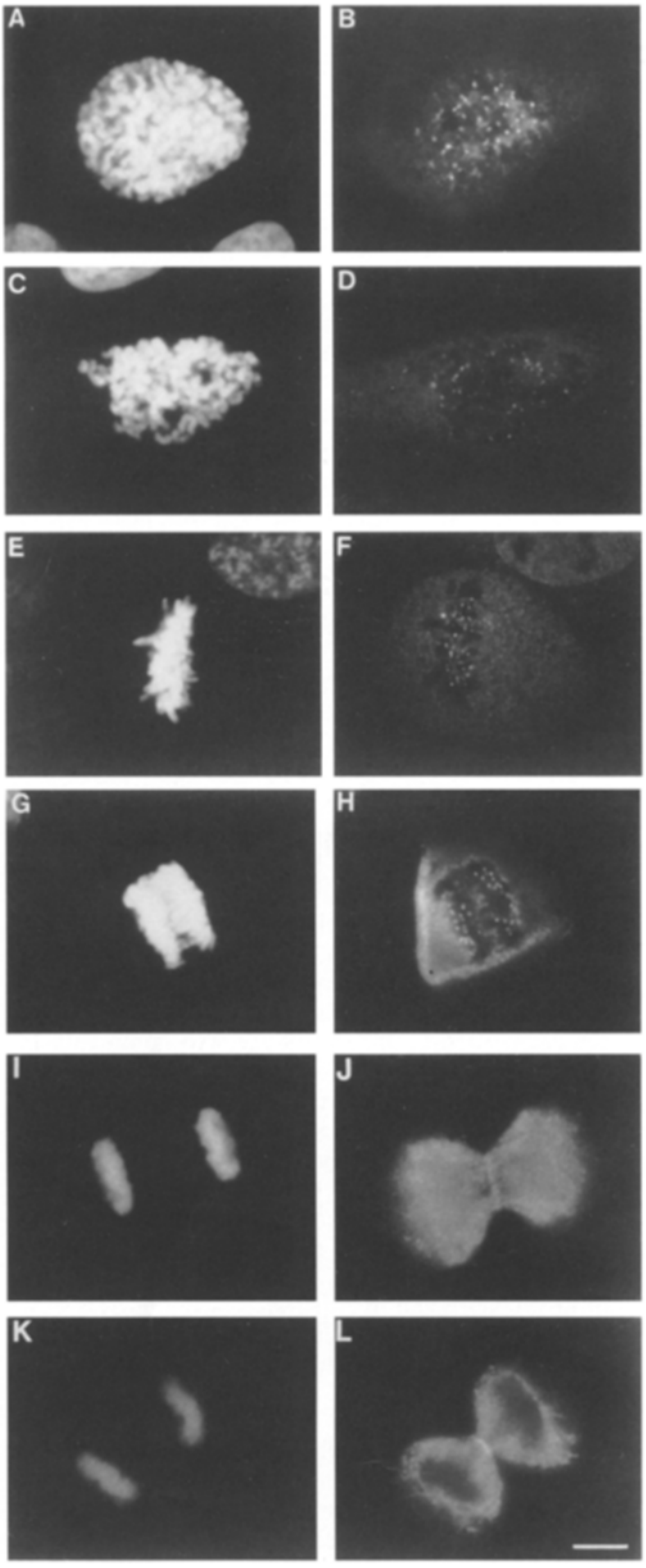

Figure 7. CENP-F is localized to different regions of the mitotic spindle at different stages of mitosis. Prophase (*A* and *B*); prometaphase (*C* and *D*); metaphase (*E* and *F*); early anaphase (*G* and *H*); late anaphase (*I* and *J*); early telophase (*K* and *L*). Chromosomes are visualized by DAPI staining (*A–F*) and anti-CENP-F IgG followed by FITC-conjugated anti-rabbit IgG (*G–L*). Bar, 10 μm.

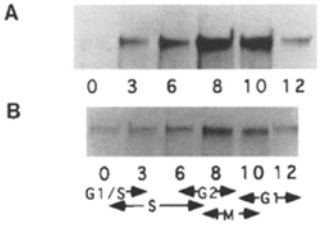

Figure 8. CENP-F expression pattern at different stages of the HeLa cell cycle. (*A*) CENP-F steady-state levels were quantitated by immunoblot analysis of equal numbers of synchronized cells at various times after release from a double thymidine block. (*B*) The synthetic rates of CENP-F at different stages of the cell cycle were measured by pulse-labeling synchronized cells for 10 min in the presence of Tran^{35}SLabel at different times after release from G1/S boundary.

with a small population (15%) of straggling G2 and M phase cells that contained stable CENP-F. This possibility was confirmed when CENP-F was found to be hyperstabilized in cells that were prevented from completing mitosis by treatment with colcemid (Fig. 9, *C* and *D*). This finding also showed that the accelerated decay of CENP-F was dependent upon progression through mitosis.

The Accelerated Decay of CENP-F Is Independent of Cytokinesis

To obtain a more accurate determination of the timing of CENP-F degradation during mitosis, we tested whether its loss was dependent upon completion of cytokinesis. G2 cells were pulse labeled and chased for four hours in control medium or medium that contained cytochalasin D to prevent cytokinesis (Fig. 10, *A* and *B*). Inhibition of cytokinesis was visually monitored by the accumulation of binucleate cells. As an internal control, we compared the rate of CENP-F decay with CENP-E (Fig. 10, *C* and *D*), a kinetochore protein whose degradation was previously shown to be insensitive to cytochalasin D (Brown et al., 1994). Comparison of CENP-E and CENP-F showed that the degradation rate (Fig. 10, *B* and *D*) of neither proteins was altered when cytokinesis was blocked. Immunofluorescence staining shows that cytochalasin D did not disrupt the localization of CENP-F at the spindle midzone in anaphase cells (Fig. 10 *E*). However, cytochalasin D-treated cells that had completed mitosis but were binucleated as a result of inhibition of cleavage furrow formation did not exhibit detectable levels of CENP-F. Thus, the localization of CENP-F to the cleavage furrow is not a prerequisite for its degradation.

Discussion

We report here the molecular characterization of human CENP-F, a kinetochore associated protein that was originally identified by a human autoimmune serum (Rattner et al., 1993). Analysis of the 10.1-kb CENP-F cDNA shows that it encodes a protein of 3211 amino acids with a calculated molecular mass of 367 kD. Authenticity of the cDNA was confirmed based on several criteria. The size of the protein encoded by the cDNA is in close agreement with the 400-kD estimate of CENP-F (Rattner et al., 1993). The autoimmune serum recognized multiple epitopes that were encoded by nonoverlapping regions of the cDNA. Antibodies generated against proteins expressed from three different regions of the cDNA identified bona

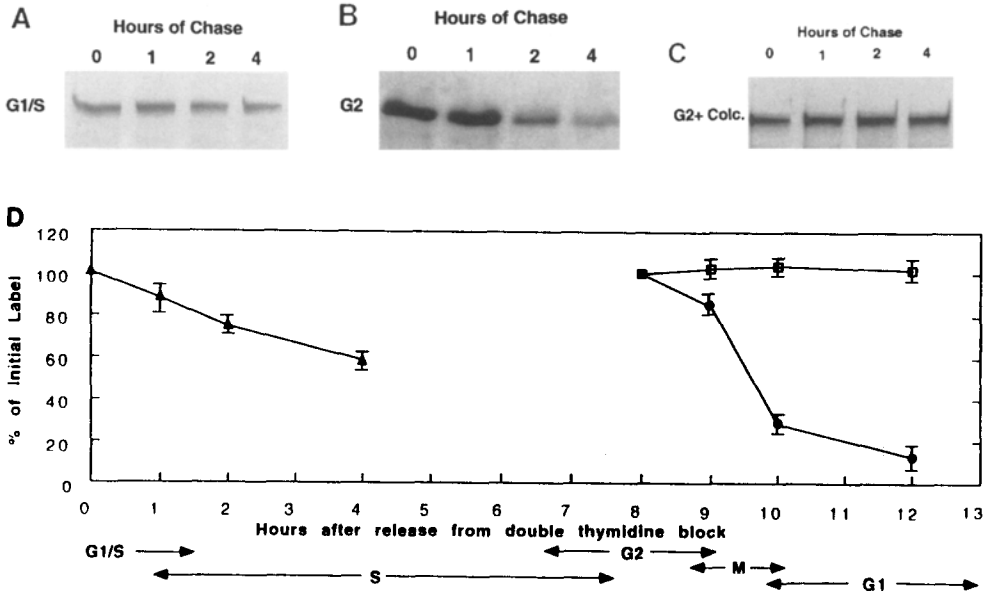

Figure 9. CENP-F decay is accelerated at the end of mitosis. (*A*) Cells synchronized at the G1/S boundary were pulse-labeled and chased in unlabeled medium for 4 h into S phase. (*B*) Pulse-chase experiment performed on cells synchronized at G2 and allowed to progress through mitosis. (*C*) Same as *B* except colcemid was included in the chase medium to block progression through mitosis. (*D*) The amount of radiolabeled CENP-F at various times of the chase were quantitated by a phosphorimager and the mean values obtained from three independent experiments are plotted as a function of the cell cycle. (—▲— represents cells pulsed in G1/S; —□— represents cells pulsed in G2; —●— represents cells pulsed in G2 in the presence of colcemid.) Error bars represent 1.96 SD units.

fide CENP-F by immunoprecipitation as well as by immunoblot analysis. Finally, these antibodies produced an immunofluorescence staining pattern that was qualitatively the same as that obtained with autoimmune sera. In an earlier report, Casiano et al. (1993) described an autoimmune serum (from patient JG) that recognizes a doublet of 330-kD proteins in HeLa cells. These proteins are associated with the nuclear matrix and exhibited a distribution pattern similar to CENP-F. It should now be possible to determine if there are CENP-F antibodies in the JG serum by testing the serum for its ability to recognize determinants encoded by the CENP-F cDNA.

Cytological and biochemical studies presented here and in our initial report (Rattner et al., 1993) highlight several unique features that distinguish CENP-F from other proteins that localize to the mammalian centromere/kinetochore. First, CENP-F is at present the largest member of the mammalian centromere family of proteins and it exhibits no significant primary sequence homologies with other proteins in the data base. CENP-F possesses two extended coil domains that flank a central core and an ATP binding motif that may be part of a mechanochemical domain. This general organization is reminiscent of some aspects of the recently described SMC family of proteins that have been implicated in chromatin compaction (Strunnikov et al., 1993; Hirano and Mitchison, 1994; Peterson, 1994; Saitoh et al., 1994). However, there are several notable differences, that include the position of the putative ATP binding site (carboxyl versus amino termini), the dissimilarity in the P-loop consensus sequence (ADIPTGKT versus GXXGXGKS), and the absence of a conserved DA box, that suggests that CENP-F is not closely related to the current SMC family. Like this family of proteins, CENP-F also appears to possess a flexible central region that may allow it to act as a hinge during certain condensation events such as the organization of the centromere–kinetochore complex during the late stages of the cell cycle.

A second unique feature of CENP-F is that it is the first kinetochore protein that has been found to be part of the nuclear matrix, an association that is most prominent at G2. Since CENP-F is not readily detected in cells at other stages of interphase, this temporary association with the matrix suggests that it is probably not essential for matrix integrity but maybe necessary for nuclear reorganization events that are associated with the onset of cell division. This cell cycle-specific function is consistent with the observation that CENP-F is rapidly degraded when cells have completed mitosis. Interestingly, we observed that at the time of nuclear matrix breakdown and the onset of chromosome condensation, CENP-F is detected at the nascent kinetochore and inner surface of the nuclear envelope. The pronounced membrane pattern may simply be due to the persistence of the nuclear matrix at the membrane during this period or it may reflect a redistribution of CENP-F to the inner surface of the membrane before nuclear envelope breakdown. It is perhaps noteworthy that CENP-F contains several clusters of consensus phosphorylation sites for cell cycle-dependent kinases. In HeLa cells, the cyclinB1/cdc2 kinase complex enters the nucleus during late G2 (Pines and Hunter, 1991) and is primarily responsible for initiating mitosis. Phosphorylation of CENP-F by the cyclinB1/cdc2 complex may be part of the mechanism that temporally regulates the distribution of CENP-F between the nuclear matrix and the kinetochores.

A third unique feature of CENP-F is that it associates with the kinetochore earlier than any other of the known transient kinetochore proteins (Brinkley et al., 1992). Its

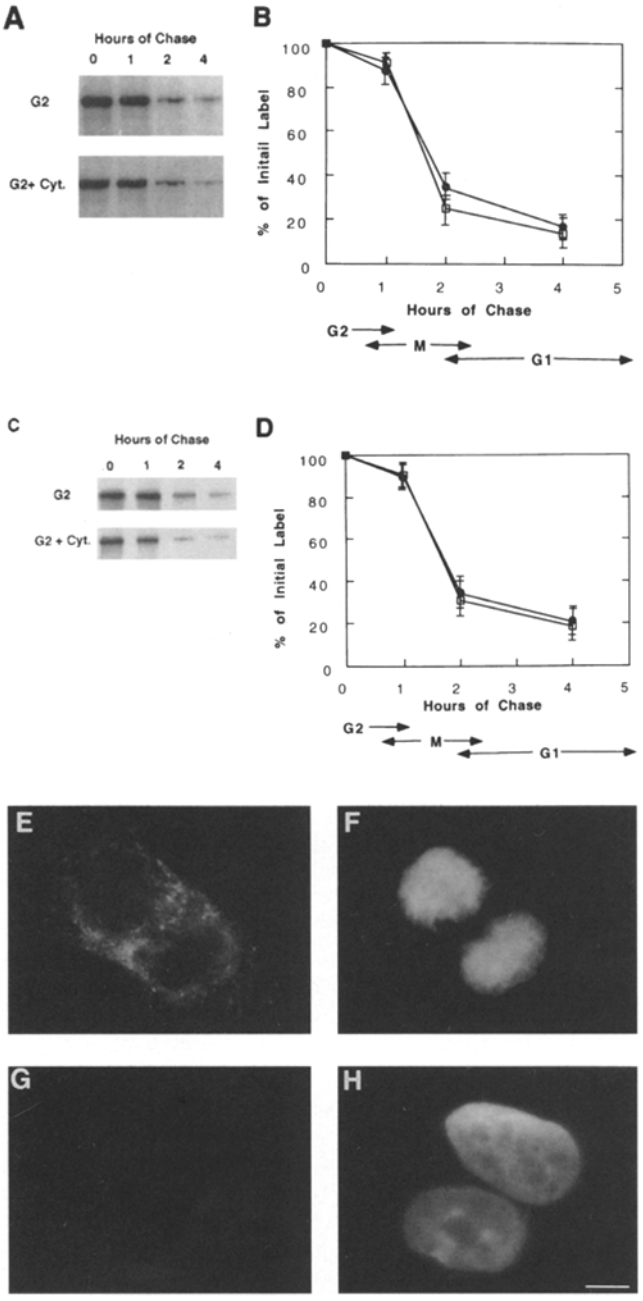

Figure 10. CENP-F degradation is independent of cytokinesis. (*A*) Cells were pulsed in late G2 and chased in the absence (*A–D*) or presence of cytochalasin D (*E–H*). (*B*) The mean values of CENP-F at each time point from three independent experiments along with their standard deviations (*error bars*) were plotted. —□—, no drug control; —●—, cytochalasin D. (*C*) CENP-E decay rates were examined in the same control (*A–D*) and cytochalasin D-treated (*E–H*) cell extracts used to determine CENP-F decay. (*D*) The mean values of CENP-E at different times from three independent experiments were plotted as in *B*. —□—, no drug control; —●—, cytochalasin D. Effect of cytochalasin D on the distribution of CENP-F in anaphase and telophase cells. Mitotic cells were harvested by shake-off, replated in the presence of cytochalasin and then processed for immunofluorescence staining with CENP-F during late anaphase (*E* and *F*) and after completion of mitosis (*G* and *H*). CENP-F staining (*E* and *G*) and the corresponding DAPI staining (*F* and *H*). Bar, 7.5 μm.

appearance at the G2 kinetochore corresponds to the period when the centromere begins its transformation from a undistinguished region of the interphase chromatin to first an amorphous electron-dense mass and then to a highly organized trilaminar kinetochore structure. The structural features of CENP-F deduced from our sequence studies (see above) and its timing of appearance at the kinetochores suggests that it may function during these early steps in kinetochore maturation. The specific spatial distribution pattern of CENP-F may explain why it does not share a higher degree of similarity with the conventional SMC family members. This prediction is partly supported by the observation that the carboxy terminus of CENP-F specifically binds to kinetochores with the same temporal pattern as the endogenous protein (Jablonski, S., and T. J. Yen, unpublished observations). Along this line, it is also noteworthy that the putative cdk phosphorylation sites that may specify when CENP-F binds to the kinetochore reside within the amino- and carboxy-terminal domains. The detection of CENP-F at kinetochores of separated chromatids in anaphase raise the added possibility that it could be important for maintaining the integrity of the kinetochore during mitosis. Thus, its degradation at the end of mitosis may be required for disassembly of the kinetochore. Although our pulse–chase data cannot precisely pinpoint when CENP-F degradation occurs during mitosis or whether certain subpopulations are degraded at different times, it remains possible that the kinetochore-bound fraction is degraded near the end of mitosis, when chromosomes begin to decondense.

A fourth feature of CENP-F is that it shows a cell cycle distribution that is both temporally regulated and diverse in terms of the structural components it localizes to. Its distribution during the latter stages of the cell cycle suggests that it could be involved in mitotic events as diverse as nuclear reorganization at G2, kinetochore maturation and function from G2 to anaphase, and intracellular bridge structure and function during anaphase–telophase. It is intriguing that under certain electrophoretic conditions, CENP-F can be resolved into two closely migrating species (Jablonski, S., and T. J. Yen, unpublished observations) that may represent different isoforms of CENP-F. We do not know whether the distribution of the two CENP-F isoforms differs since our antibodies recognize both forms and may produce the complex distribution pattern observed for CENP-F. It is possible that specific isoforms are found in association with the nuclear matrix, kinetochore and intercellular bridge.

Finally, CENP-F joins an increasing number of proteins that localize to the spindle midzone and the intracellular bridge at anaphase and telophase, respectively (Fishkind and Wang, 1995). Whether CENP-F interacts with some of these proteins to participate or coordinate cleavage furrow formation remains to be addressed. Since the inhibition of cleavage furrow formation does not affect the decay of CENP-F, the localization of this protein to this structure is not part of the pathway towards its degradation.

The authors express their thanks to D. He for advice on preparing nuclear matrix; B. T. Schaar for bringing our attention to SMC proteins; and S. Jablonski and G. Chan for sequence analysis and reading of our manuscript. Special thanks to the staff members at the LAF for animal work and Special Services for reproduction of figures and G. Waters and S. Gill

for assistance with the COILCOIL program. We also acknowledge W. H. Lee for providing us with the unpublished sequence information from their partial CENP-F cDNA.

T. J. Yen is a Scholar of the Lucille P. Markey Charitable Trust, and this work was supported by the Markey Charitable Trust, Council for Tobacco Research, National Institutes of Health grant GM-44762, USPHS core grant CA-06927 and an appropriation from the Commonwealth of Pennsylvania. J. B. Rattner is supported by the Canadian Cancer Institute with funds from the Canadian Cancer Society and the Medical Research Council of Canada. G. Mack is supported by the Alberta Heritage Foundation for Medical Research.

Received for publication 3 May 1995 and in revised form 8 May 1995.

References

Altschul, S. F.,W. Gish, W. Miller, E. W. Myers, and D. J. Lipman. 1990. Basic local alignment search tool. *J. Mol. Biol.* 215:403–410.

Bernat, R. L., G. G. Borisy, N. F. Rothfield, and W. C. Earnshaw. 1990. Injection of anticentromere antibodies in interphase disrupts events required for chromosome movement at mitosis. *J. Cell Biol.* 111:1519–1533.

Bernat, R. L., M. R. Dennoy, N. F. Rothfield, and W. C. Earnshaw. 1991. Disruption of centromere assembly during interphase inhibits kinetochore morphogenesis and function in mitosis. *Cell.* 66:1229–1238.

Brenner, S., D. Pepper, M. W. Berns, E. M. Tan, and B. R. Brinkley. 1981. Kinetochore structure, duplication, and distribution in mammalian cells: analysis by human autoantibodies from Scleroderma patients. *J. Cell Biol.* 91:95–102.

Brinkley, B. R., I. Ouspenski, and R. P. Zinkowski. 1992. Structure and molecular organization of the centromere-kinetochore complex. *Trends Cell Biol.* 2: 15–21.

Brown, K. D., R. M. Coulson, T. J. Yen, and D. W. Cleveland. 1994. Cyclin-like accumulation and loss of the putative kinetochore motor CENP-E results from coupling continuous synthesis with specific degradation at the end of mitosis. *J. Cell Biol.* 125:1303–1312.

Casiano, C., G. Landberg, R. L. Ochs, and E. M. Tan. 1993. Autoantibodies to a novel cell cycle-regulated protein that accumulates in the nuclear matrix during S phase and is localized in the kinetochores and spindle midzone during mitosis. *J. Cell Sci.* 106:1045–1056.

Clarke, L., and J. Carbon. 1985. The structure and function of yeast centromeres. *Annu. Rev. Genet.* 19:29–56.

Doheny, K. F., P. K. Sorger, A. A. Hyman, S. Tugengreich, F. Spencer, and P. Heiter. 1993. Identification of essential components of the *S. cerevisiae* kinetochore. *Cell.* 73:761–774.

Earnshaw, W. C., and N. Rothfield. 1985. Identification of a family of human centromere proteins using autoimmune sera from patients with Scleroderma. *Chromosoma.* 91:313–321.

Endow, S. A., S. J. Kang, L. L. Satterwhite, M. Rose, V. P. Skeen, and E. D. Salmon. 1994. Yeast Kar3 is a minus-end microtubule motor protein that destabilizes microtubules preferentially at the minus ends. *EMBO J.* 13:2708–2713.

Fishkind, D. J., and Y. Wang. 1995. New horizons for cytokinesis. *Curr. Opin. Cell Biol.* 7:23–31.

Fry, D. C., S. A. Kuby, and A. S. Mildvan. 1986. ATP-binding site of adenylate kinase: Mechanistic implications of its homology with *ras*-encoded p21, F_1ATPase, and other nucleotide-binding proteins. *Proc. Natl. Acad. Sci. USA.* 83:907–911.

Goh, P., and J. V. Kilmartin. 1993. NCD10: a gene involved in chromosome segregation in *Saccharomyces cerevisiae*. *J. Cell Biol.* 121:503–512.

He, D., J. A. Nickerson, and S. Penman. 1990. Core filaments of the nuclear matrix. *J. Cell Biol.* 110:569–580.

Hirano, T., and T. J. Mitchison. 1994. A heterodimeric coiled-coil protein required for mitotic chromosome condensation in vitro. *Cell.* 79:449–458.

Hyman, A. A., K. Middleton, M. Centola, T. J. Mitchison, and J. Carbon. 1992. Microtubule-motor activity of a yeast centromere-binding protein complex. *Nature (Lond.).* 359:533–535.

Jiang, W., L. Lechner, and J. Carbon. 1993. Isolation and characterization of a gene (CBF2) specifying a protein component of the budding yeast kinetochore. *J. Cell Biol.* 121:513–520.

Lechner, J., and J. Carbon. 1991. A 240 Kd multisubunit protein complex, CBF3, is a major component of the budding yeast centromere. *Cell.* 64:717–725.

Linder, P., P. F. Lasko, M. Ashburner, L. Leroy, P. J. Nielsen, K. Nishi, J. Schnier, and P. P. Slonimski. 1989. Birth of the D-E-A-D box. *Nature (Lond.).* 337:121–122.

Lupas, A., M. Van Dyke, and J. Stock. 1991. Predicting coiled coils from protein sequences. *Science (Wash. DC).* 252:1162–1164.

Middleton, K., and J. Carbon. 1994. Kar3-encoded kinesin is a minus-end-directed motor that functions with centromere binding proteins (CBF3) on an *in vitro* yeast kinetochore. *Proc. Natl. Acad. Sci. USA.* 91:7212–7216.

Moroi, Y., A. L. Hartman, P. K. Nakane, and E. M. Tan. 1981. Distribution of kinetochore (centromere) antigen in mammalian cell nuclei. *J. Cell Biol.* 90: 254–259.

Peterson, C. L. 1994. The SMC family: novel motor proteins for chromosome condensation? *Cell.* 79:389–392.

Pfarr, C. M., M. Coue, P. M. Grissom, T. S. Hays, M. E. Porter, and J. R. McIntosh. 1990. Cytoplasmic dynein is localized to kinetochores during mitosis. *Nature (Lond.).* 345:263–265.

Pines, J., and T. Hunter. 1991. Human cyclins A and B1 are differentially located in the cell and undergo cell cycle-dependent nuclear transport. *J. Cell Biol.* 115:145–153.

Rattner, J. B., J. Lew, and J. H. Wang. 1990. $p34^{cdc2}$ kinase is present at several distinct domains within the mitotic apparatus. *Cell Motil. Cytoskeleton.* 17: 227–235.

Rattner, J. B., A. Rao, M. J. Fritzler, D. W. Valencia, and T. J. Yen. 1993. CENP-F is a *.ca 400 KDa* kinetochore protein that exhibits a cell-cycle dependent localization. *Cell Motil. Cytoskeleton.* 26:214–226.

Saitoh, N., H. G. Goldberg, E. R. Wood, and W. C. Earnshaw. 1994. ScII: an abundant chromosome scaffold protein is a member of a family of putative ATPases with an unusual predicted tertiary structure. *J. Cell Biol.* 127:303–318.

Sambrook, J., E. F. Fritsch, and T. Maniatis. 1989. Molecular cloning: a laboratory manual 2nd ed., Vol. 1. Cold Spring Harbor Laboratory, Cold Spring Harbor, NY.

Saraste, M., P. R. Sibbald, and A. Wittinghofer. 1990. The P-loop- a common motif in ATP- and GTP-binding proteins. *Trends Biochem. Sci.* 15:430–434.

Staufenbiel, M., and W. Deppert. 1984. Preparation of nuclear matrices from cultured cells: subfractionation of nuclei in situ. *J. Cell Biol.* 98:1886–1894.

Steurer, E. R., L. Wordeman, T. A. Schroer, and M. P. Sheetz. 1990. Localization of cytoplasmic dynein to mitotic spindles and kinetochores. *Nature (Lond.).* 345:266–268.

Strunnikov, A. V., V. L. Larionov, and D. Koshland. 1993. *SMC1*: an essential yeast gene encoding a putative head-rod-tail protein is required for nuclear division and defines a new ubiquitous protein family. *J. Cell Biol.* 123:1635–1648.

Walker, J. E., M. Sarste, M. J. Runswick, and N. J. Gay. 1982. Distantly related sequences in the α- and β-subunits of ATP synthase, myosin, kinases and other ATP-requiring enzymes and a common nucleotide binding fold. *EMBO J.* 1:945–951.

Yen, T. J., D. A. Compton, D. Wise, R. P. Zinkowski, B. R. Brinkley, W. C. Earnshaw, and D. W. Cleveland. 1991. CENP-E, a novel human centromere-associated protein required for progression from metaphase to anaphase. *EMBO J.* 10:1245–1254.

Yen, T. J., G. Li, B. Schaar, I. Szilak, and D. W. Cleveland. 1992. CENP-E is a putative kinetochore motor that accumulates just before mitosis. *Nature (Lond.).* 359:536–539.